HHS Public Access

Author manuscript

Semin Cell Dev Biol. Author manuscript; available in PMC 2021 July 12.

Published in final edited form as:

Semin Cell Dev Biol. 2020 April ; 100: 212–222. doi:10.1016/j.semcdb.2019.11.005.

Viscoelastic voyages – biophysical perspectives on cell intercalation during *Drosophila* gastrulation

Dinah Loerke[1,*], **J. Todd Blankenship**[2,*]

[1]Department of Physics and Astronomy, University of Denver, Denver, CO 80208, USA.

[2]Department of Biological Sciences, University of Denver, Denver, CO 80208, USA.

Abstract

Developmental processes are driven by a combination of cytoplasmic, cortical, and surface-associated forces. However, teasing apart the contributions of these forces and how a viscoelastic cell responds has long been a key question in developmental biology. Recent advances in applying biophysical approaches to these questions is leading to a fundamentally new understanding of morphogenesis. In this review, we discuss how computational analysis of experimental findings and *in silico* modeling of *Drosophila* gastrulation processes has led to a deeper comprehension of the physical principles at work in the early embryo. We also summarize many of the emerging methodologies that permit biophysical analysis as well as those that provide direct and indirect measurements of force directions and magnitudes. Finally, we examine the multiple frameworks that have been used to model tissue and cellular behaviors.

Keywords

biophysics; developmental biology; morphogenesis; cell intercalation; gastrulation

1. Introduction

The last decade has seen a biophysical revolution in biological research, with new microscopy, computational and cell biological-based approaches being harnessed to advance the physical understanding of cellular processes. These approaches have revealed the combined viscous (or frictional resistance to deformation) and elastic (the ability to return to an original state after deformation) properties of biological tissues and cells, and the potentially different timeframes that these viscoelastic properties may operate within. Along with these experimental approaches, *in silico* modeling has provided a means to test which systematic properties define and are able to predict behaviors *in vivo*. Here, we will touch on some of the key advances and literature that have helped to define this new approach to studying the development of the early fly embryo. Although we discuss many of the central

*Authors for correspondence: dinah.loerke@du.edu; todd.blankenship@du.edu.

studies that have introduced important new biophysical advances, we apologize in advance to authors of relevant literature that we did not have space to discuss.

Epithelial morphogenesis during Drosophila gastrulation

During gastrulation in the *Drosophila* embryo, the central morphological changes can largely be categorized as processes that, 1) cause a remodeling of tissue dimensions through anterior-posterior axis elongation, or 2) create folds or furrows in the monolayered epithelium (Fig. 1a). The processes that drive axis elongation are mainly reliant on changes in topological relationships that direct neighbor exchange along the anterior-posterior (AP) axis, although there are contributions from other processes as well. The folding processes that occur during gastrulation lead to the movement of cells into the interior of the embryo. In some cases, these furrows will be transient in nature, and eventually cells will return to the surface epithelium (e.g., the cephalic furrow and dorsal folds), but in other cases this is a mechanism for permanently relocating cells into basal layers (ventral furrow and midgut invaginations). Of these furrowing processes, the invagination of the mesoderm through the formation of the ventral furrow has been a classic system for understanding how cells can coordinate the adoption of a common, conical topology to drive furrow formation. Work on the mechanisms of axis elongation, or germband extension (GBE), and ventral furrow formation have helped to redefine how development is studied through the incorporation of biophysical principles and approaches. However, in this review we will mainly concentrate on axis elongation as an example of how these approaches are changing the way that developmental processes are studied.

Cell intercalation and tissue elongation

During axis elongation in the early fly embryo, the germband epithelium - comprising approximately the posterior and ventrolateral two thirds of the *Drosophila* embryo - will undergo a doubling in length over the course of two hours of development. This elongation of the main AP axis occurs with a compensatory narrowing of the germband along the dorsoventral (DV) perpendicular axis. The majority of extension occurs in only 30 minutes, demonstrating the speed of the process. Formally, there are four morphological processes that commonly direct changes in tissue dimensions when they occur in an oriented fashion: 1) cell intercalation, 2) cell migration, 3) cell division, and 4) elongation of individual cell dimensions. The main driver during this first, fast phase of germband extension is cell intercalation, with minor contributions from anisotropic changes in cell areas as well as oriented cell divisions [1], [2], [3], [4]. It is also possible that cell migration may occur during axis elongation in the fly embryo [5]. It is interesting to note that, although intercalation is the primary driver, each of these processes is potentially harnessed during axis elongation. This may again reflect the necessity for rapid development in the early *Drosophila* embryo.

Cell intercalation in the germband occurs through the contraction of interfaces between neighboring cells along the AP axis (sometimes referred to as “T1 interfaces”) (Fig. 1b). This contraction of vertically-oriented interfaces produces neighbor exchange among four-cell groups of cells (T1 transitions) or among larger numbers of cells (rosettes) (Fig. 1b) [6], [7]. Interface contraction brings cells together in a common point (T2 junctions, or the

vertex stage of rosette formation), after which new interface growth resolves this structure into an array of cells that is elongated along the AP axis (T3 junctions, rosette resolution) and thus driving overall extension of the tissue.

Cytoskeletal and adhesion proteins involved in force transmission and generation

The reshaping of tissue architecture requires the function of apical and junctional proteins [6], [7], [8]. These proteins, in addition to their essential roles in the establishment of cell adhesion and apical-basal polarity, are utilized in a system of polarity that is oriented within the plane of the epithelial sheet. This planar polarity operates to drive cell intercalation and generates asymmetric distributions of cytoskeletal and adherens junction proteins. The Bazooka/PAR-3 PDZ-domain protein and the adherens junction proteins E-Cadherin and Armadillo/ß-catenin are concentrated at interfaces between dorsal and ventral neighbors (DV interfaces) [7], [8]. Conversely, filamentous actin (F-actin) and the actin-based Myosin II motor protein are enriched in the reciprocal AP interfaces [6], [7], [8]. Contractile Myosin II proteins are also found in several additional populations in the early embryonic epithelium – one population is present in the apical/medial cap of intercalating cells where it mediates oscillations in cell area [9], [10], [11], while a third population is present as strong enrichments along with E-cadherin at cell vertices [12]. These planar polarities are extraordinarily dynamic, with initial planar polarization occurring in 15 minutes of development, and can be measured with automated, quantitative tools [13].

2. Observing cell behaviors during gastrulation

Epithelial morphogenesis as a pulsatile process

One of the major advances in studying developmental biology has been the adoption of live imaging techniques that permit the rapid imaging of cell and tissue morphologies. With faster acquisition times, it became possible to resolve morphological processes with high spatiotemporal resolution. Notably, spinning disc confocal microscopy became a staple in imaging *Drosophila* gastrulation events. With these new imaging capabilities came major changes in understanding how these processes occurred. A central feature of this was the demonstration that these developmental processes are not continuous, but instead occur in pulses [9], [10], [11], [14]. Indeed, events such as interface shrinkage, apical constriction, and Myosin II recruitment were each shown to have periodic behaviors, in which cells cycled between active phases and inactive or reversing phases. In general, these pulses were observed to occur on a minutes timescale, with individual active periods of approximately 45–90 seconds in length [9], [10], [11], [12], [14].

Computational approaches to measuring cell dimensions and protein intensities

With increased temporal resolution, time-lapse imaging began to produce data sets that can comprise several thousand individual images. This imaging complexity meant that it became increasingly difficult to apply manual approaches of quantitation. This led to the development of automated methods to identify cells and extract relevant features, such as cell-cell junctions. Another important property of automated analysis is that it removes the potential for user bias that may occur in manual measurements. To this end, it has become standard practice to employ Matlab encoded algorithms to segment (or recognize) individual

epithelial cells in images from gastrulating embryos, although users are increasingly shifting to other computer languages such as Python.

A general work flow for computational analysis usually involves the application of a filter to raw data to reduce noise (Fig. 2). Typical filters that are employed are Gaussian, high pass, or denoising filters, followed by masking of regions that are not of interest. A seeded watershed algorithm is then used to grow cell areas from regions of local intensity minima which then results in the recognition of cell boundaries [10], [15], [16]. Alternative approaches have used image processing and thresholding to achieve boundary recognition [17], [18]. This process of segmentation is then applied iteratively on each image file, and tracking across time is implemented based on the degree of overlap between individual cells. The resulting “skeletonized” and tracked representation of the tissue yields a wealth of information, from cell areas and perimeters to interface contours, lengths and orientation angles which can be further analyzed. Additionally, protein intensities at cell interfaces can be calculated from a second imaged channel, or regions of interest can be defined based on distances from discrete objects such as cell vertices, interfaces or centroids. Several software packages have been made freely available that accomplish the process of segmentation and tracking from raw data (SIESTA, TissueMiner, SEGGA, and others) [10], [18], [19].

The direct results of seeded watershed algorithms are fairly robust, but often require manual correction to obtain the desired level of accuracy. This is often because the initial seeding process either under- or over-seeds individual cells. Various approaches have addressed this problem by linking tracking with seeding and by propagating seeds from timeframe to timeframe. For example, the overall flow of the tissue can be used to displace seeds in a predictive manner [4], [12]. It will be interesting to see if new artificial intelligence-driven approaches can improve processing times and quality. As an example of this, machine-learning has been successfully applied to detect cell divisions in the germband using a training set of 90 cells and 14 measured features [4]. Through this approach, the authors found that a narrow band of cells adjacent to the ventral furrow undergo oriented cell divisions that help to relieve strain in the absence of cell intercalation.

Determining active motion within the context of pulsed processes

As force generation during gastrulation is pulsatile, determining periods of active, stepped motion is critical to understanding how force profiles change in different genetic and tissue contexts. While early approaches relied on making manual decisions on what constituted a contractile step, analyzing mean squared displacement-based curves permits a quantitative and unbiased determination of periods of active motion (Fig. 3). This approach builds on standard methods used across many fields to isolate periods of active movement versus other forms of motion by measuring mean squared displacements (MSDs). Once MSDs are determined, they are fit to an MSD function that has constrained, diffusive, and active components. To detect active motion steps a rolling window analysis technique is often used [20]. Given the high variability in pulsed behaviors, one of the challenges of a rolling window method is in selecting the size of the window [9], [10], [11], [12]. A window too large will make detecting brief steps unlikely, whereas a window too short will perform

worse at detecting longer steps. Thus, adopting a rolling window with variable widths optimized for the step sizes in a particular system becomes important.

Interpreting cell behaviors based on phase

An additional issue with analyzing data from oscillatory systems that possess high variable periods is isolating productive contractile events. Breaking down oscillatory cycles into phases can permit the analysis of individual contractile and expansion behaviors. To obtain instantaneous phase measurements of an oscillating signal such as cell area, an osculating circle method (based on performing a Hilbert transform) can be used [21]. Similar to how images were filtered prior to segmentation, oscillation traces are filtered to remove temporal noise that could result in artificially high frequency oscillations. At the end of this process, an area phase space is generated that permits the examination of cell behaviors in relation to the individual contractile and expansive components of a cell's oscillatory cycle. This can be very useful in assessing how area contractions impact the shrinkage of T1 interfaces and the displacements of adjacent tricellular vertices [12].

3. Methods to examine forces in the embryonic epithelium

The central question that drives much research on morphogenesis is the determination of where and when cells produce forces. This can be a difficult question to address, particularly in a system like the early fly embryo, in which an intact organism with an overlaying eggshell-like membrane (the vitelline membrane) poses an impediment to direct mechanical interventions. To date, the primary means of identifying differential force application in the fly embryo have been to laser cut cell interfaces, or to use inferred stress approaches based on deformations of cellular dimensions, but other approaches are also being pioneered. We will discuss several of these approaches in the following section.

Laser-directed microcutting:

The first of these approaches to be applied to intercalation in the fly embryo was to cut cell interfaces or cortical networks using focused laser ablations [17], [22]. The recoil rates of the cell vertices associated with the cut interfaces can be tracked and thus relative tensions can be inferred from these displacements. By using these methods, it has been determined that interfaces between AP neighboring cells experience higher tensions based on the observation of higher recoil rates after laser ablation. This led to the canonical model of interface-spanning line tensions that drive interface contraction and thus the remodeling of cell topologies [9], [17], [22]. Interestingly, another recent use of cutting lasers has been to cauterize epithelial cells to the vitelline membrane. Through this approach, it was possible to immobilize one end of the germband and test if the growth of new T3 interfaces was a passive effect of tissue relaxation or an active process [23]. New interfaces were observed to still extend after cauterization, although they became aberrantly oriented. This offered the key insight that interface extension is driven by an active process at the level of individual cells, but that tissue relaxation directed by the invagination of the posterior midgut aids the directionality of the process. The strength of laser ablation as a tool can be further observed in that it can target subcellular structures. Myosin II is enriched in the middle of the apical cortex as well as in junctionallyassociated populations. Laser ablation has been used to

individually ablate apical/medial structures in the anterior or posterior cells abutting a newly growing interface. Interestingly, this halted interface growth, while cutting junctional or medial pools in the DV-juxtaposed cells sharing the growing interface had little effect [23], [24]. These results demonstrated that an active pulling force from the cells at the end of each growing T3 interface are, at least in part, responsible for the force generation driving T3 transitions.

Inferred stress approaches:

Strain rate analysis represents another approach to understanding where forces originate from, and how they lead to the deformation of tissue and cell shapes. Flow patterns based on cell centroid velocities can be used to generate overall tissue tensors, while more local measurements of cell deformations can lead to determinations of cell shape strain rates [3], [25]. By subtracting tissue and cell strain rates, an evaluation of the relative impacts of processes such as cell intercalation on overall tissue morphogenesis can be calculated. Using this approach, Butler et al. [3] found that changes in cell shape contributed to changes in tissue dimensions during germband extension. They further found that intercalation defects in Krüppel AP patterning mutants could be partially compensated by increased elongation of cells in the AP direction. Recent work has extended this image-based calculation of stresses by using a mechanical inference model and then validating it against recoil velocities from laser ablation experiments [26]. These stresses were also found to correlate well with regions of Myosin II intensity, the primary generator of cytoskeletal force in the early embryo. By using this approach, a calculation of shear stresses at individual junctions was obtained. Given these results, the individual contributions of medial and junctional Myosin II could be measured, and the overall stresses that lead to either E-cadherin stabilization or destabilization were determined. The anisotropy of tensions at contracting interfaces was then proposed to lead to shear forces that destabilize these interfaces.

Particle tracking velocimetry:

Although the contribution of actomyosin forces to *Drosophila* morphogenesis is well-appreciated [27], understanding how these forces are transmitted requires an analysis of the viscoelastic properties of the cell. One of the foundational studies on this examined formation of the ventral furrow [28]. To explore how apically-generated actomyosin forces propagated through a viscous cytoplasm, He et al. [28] employed particle tracking velocimetry (often referred to as PIV). However, unlike in many circumstances in which local inhomogeneities in protein localization (filamentous actin, membrane markers) are used to infer flow patterns, 500-nm polystyrene fluorescent microspheres were injected as passive trackers of cytoplasmic movements. Using this data, it became apparent that laminar-like flows occurred in which constriction of the apical cortex by actomyosin forces appeared to drag the underlying cytoplasm. They then could model these movements using Stokes equations to predict viscous flows at low Reynolds numbers. As apical surfaces contract in cells of the ventral furrow there is a concomitant lengthening of the cells. The authors observed a close agreement between the predicted viscous flows and cell lengthening rates, suggesting that forces at the plasma membrane had little contribution to cell lengthening. Surprisingly, laminar flows also often appeared to be beyond the scale of individual cells. To address this, the authors examined if the functional unit of apical

constriction and cell lengthening occurs at a supracellular level by observing cytoplasmic movements in an acellular context. Using mutations that block cellularization, they observed that embryos that lacked cells still displayed very similar flow patterns to wild-type embryos with only a slight reduction in flow rates. Remarkably, this suggests that hydrodynamic properties of the early embryo can direct major properties of tissue movements at a supracellular scale and shows how viscous characteristics of a tissue system can drive developmental events.

Rheological measurements using ferrofluids:

Building on the above studies, a new approach to directly measure viscoelastic cellular properties has been to embed ferrofluids in embryos and then analyze their deformation and displacement when placed in a magnetic field [28], [29], [30], [31], [32]. Using this approach during cellularization, the epithelial-forming process just prior to gastrulation, Doubrovinski et al. [30] found that the cytoplasm was predominantly viscous in character, albeit with a viscosity ~1000× more viscous than water. By contrast, the cell cortex had elastic properties which were largely reliant on the dynamics of the filamentous actin cytoskeleton, thus showing that distinct elements of total cellular viscoelasticity are derived from different physical spaces. The measured elastic properties had relaxation times that were on the minutes time scale with a reported lower bound of 4 minutes. This is intriguing, as relaxation times of this order are compatible with the minutes timescales at which gastrulation events occur. Interestingly, a study using microrheological measurements of injected fluorescent beads came to similar conclusions on the viscous properties of cellularizing embryos, but also implicated microtubule networks located near the nuclei and cell cortex with local increases in both elastic and viscous moduli [33]. These studies were performed just prior to GBE; it will be interesting to see what future studies using ferrofluids and performed during active cell intercalation reveal.

Using optical tweezers to probe force dissipation:

A further examination of the viscoelastic properties of epithelial cells during cell intercalation examined the temporal dynamics of force dissipation [34]. As force generation is pulsatile, to achieve an irreversible change in cell shape the elastic properties of the cells must be overcome and a viscous response occur which will then permit a lasting deformation. The authors hypothesized that cell interfaces would possess a short-term elastic response and a long-term viscous response due to force dissipation. They further posited that cortical filamentous actin would control the dissipation of elastic forces. To examine this, they first analyzed the reversibility of cell shape changes generated by different durations of Myosin II contractile pulses. They found that the longer the pulse, the more irreversible the effect on interface length. To induce their own controlled-length pulses, they introduced the use of optical tweezers. Again, they found that longer pulling times on cell interfaces led to a higher degree of irreversibility in cell shape changes. Finally, to examine if filamentous actin is a major determinant of the elastic response they injected low-levels of Cytochalasin D, which inhibited actin turnover. In this context, stabilizing filamentous actin led to a greater elastic response and a higher degree of reversibility. These results again supported their model that elastic properties of epithelial cells are capable of relaxing on the order of a few

minutes, and suggest that Myosin II activity could aid in the fluidization of actin filaments and force dissipation by promoting filament turnover.

4. Biophysical interpretations of the motive forces for tissue elongation in *Drosophila*

Line tensions and vertex displacements

Previous research into the positional cues that direct oriented intercalation has shown that AP patterning information is translated into asymmetric protein distributions at the cellular level [6], [7], [8]. As discussed above, at AP interfaces Myosin II forms both supracellular cables and smaller, transient networks, and AP cell interfaces that were cut by laser ablation showed higher recoil velocities than DV cell interfaces (Fernandez-Gonzalez et al., 2009; Rauzi et al., 2008). This body of work led to what has been the dominant model for cell intercalation, where planar polarized actomyosin networks mediate higher line tensions at AP interfaces, and these higher tensions drive contraction of the associated cell interfaces [17], [22]. Line tension-based models have also been the main means of computationally modeling epithelial cell intercalation (discussed below). It is interesting to note that increased tension, applied through a suction technique, has been shown to function through a positive feedback loop to further recruit Myosin II [22]. This suggests that local tension can enhance force production. However, the mechanism by which these interface-localized tensions drive interface contraction has been less clear. Unbalanced tensions on either side of a cell interface could drive shear forces that would lead to the destabilization of cell-cell adhesion complexes [26]. Alternatively, Myosin II activity has been shown to drive clustering of adhesion complexes that are then endocytosed, thus producing lower adhesion forces at AP interfaces [35]. This endocytosis occurs through large Rab35 positive tubular invaginations that have lifetimes similar to the periodic contractile pulses in the germband [16]. Interestingly, Myosin II activity is essential to the termination of these compartments and cell ratcheting is disrupted after Rab35 function is compromised [16]. Thus, there are many potential mechanisms that may explain how interface-associated Myosin II and/or line tensions could direct the contraction of T1 interfaces.

Physical coupling of cell vertices and vertex sliding

Recent work has re-examined aspects of these line tension models (Fig. 4) [12]. One fundamental expectation of these models is that the motion of tricellular vertices connected by contracting interfaces should demonstrate physical coupling. Surprisingly, this was not observed, and instead cells during tissue elongation are radially coupled, with cell vertices that are most directly opposed from each other across the cell showing coordinated contractile movements. This suggests that the strongest, detectable motive force in cells at these stages are the oscillatory contractions in cell area and further suggests that tricellular vertices could be a key functional unit directing cell intercalation. It is interesting to note that medial actomyosin networks are found in a variety of epithelial morphogenetic processes and drive tissue shaping events by mediating oscillations in cell area [14], [36], [37], [38]. Using a phase-based analysis, Vanderleest et al. [12] could observe systematic changes in interface lengths with respect to cell area oscillations. Interestingly, a larger than

isotropic decrease in vertical interface lengths occurred during area contraction, and were preserved during the subsequent expansion in cell areas during an oscillatory cycle. Conversely, adjacent, non-vertical interfaces underwent a smaller than isotropic decrease in interface length, and had a compensatory increase in interface length during area expansion. These results are consistent with tricellular vertices displacing through a sliding mechanism, akin to a zippering motion, and suggest a new, alternative mechanism based on independent vertex motions as a basis for interface contraction.

5. Modeling cell intercalation

Computational models provide a framework for analysis and prediction

In its most basic form, any quantitative model, such as a simple mechanical model, provides a quantitative framework in which experimental data can be interpreted and analyzed, and it allows the development of an abstract representation of the biological system of interest (Table 1). On the upper end of the spectrum, rigorous quantitative and computational models strive to produce a fully functional 'toy' model of the system of interest. In the specific instances we will discuss here, these models will generate an implementation of an epithelial sheet that evolves its shape over time in a fashion that mimics the biological system. Any model is necessarily a simplification, and the required level of fine-graining in the model will depend on the question of interest – what they have in common is that they need to macroscopically recapitulate the feature of interest (e.g. tissue convergent extension or furrow formation). Ideally, the toy model should be validated using experiments; conversely, an effective model can be used to test competing hypotheses about the biological systems, and to formulate new predictions about the behavior of the system of interest which can then be tested experimentally [39].

Cell-based models allow the incorporation of cell-level regulation

In the field of epithelial biology, there are important and useful applications of continuum model descriptions of epithelial sheets; for example, two-dimensional hydrodynamic sheets. These models assume a homogeneous tissue with macroscopic elastic moduli (which do not require and mostly do not include any resolution of the cellular structure) that can be used to examine rheology, macroscopic deformations of the tissue such as sheet bending, and lateral deformations such as extension or shear. The advantage of describing epithelial sheet deformations within the standard theory of continuum mechanics is its mathematical tractability – with some simplifications and boundary conditions, this approach can yield analytical solutions to the relevant differential equations that characterize the deformation of the sheet, so that it produces equations that predict shapes or shape changes.

In contrast, cell-based models (including both cellular Potts models and vertex models) treat and model cells as separate and unique entities, and thus incorporate mechanical properties at the cellular level, which are potentially linked to the function of cytoskeletal and adhesion proteins (Fig. 5). Cell-based models overall are less amenable to mathematical analysis than continuum models. As a result, some studies have tried to bridge this gap by combining discretization at the cellular level with hydrodynamic models. For example, one recent study [40] used a two-dimensional hydrodynamic model of epithelia that includes a field

representing coarse-grained cell shape, which can thus differentiate between cell shape change and topological transitions. Another study [41] used a model where mechanical properties of cells are described through two parameters that represent the balance between adhesion and contractility, but in which the epithelium is macroscopically described by a continuum mechanics approach. This allowed it to address independent macroscopic bending and shear deformations of the tissue. Recent work also used a hybrid cell-based model that focuses on the viscosity contribution to macroscopic deformation [42]. However, most of the cell-based models discussed in the following do not pursue large-scale analytical solutions to the differential equations through incorporating some type of continuum model approach, but instead perform the equivalent of finite element numerical approaches [43], by solving the equations separately in individual small subunits (e.g. individual cells or subcellular elements).

While we will focus here on vertex models (and their variants), it should be mentioned that cellular Potts models have also been used successfully for modeling cell intercalation, and were among some of the first modeling approaches used in the study of intercalation. In these cellular Potts models, cells are represented computationally by a collection of pixels, allowing round and irregular shapes. The time evolution of the tissue configuration works through pixels changing their ‘cellular’ identity based on a set of rules that seeks to optimize an energy term. With these modeling approaches, it has been shown that cell intercalation can be produced solely through the introduction of planar polarity of cell-cell adhesion [44], [45].

Vertex models for epithelial sheets capture cell shape, physical tensions, and adhesion

Vertex models, which are widely used for epithelial sheets, are simplified descriptions of tissue configurations that nevertheless are thought to capture the most relevant features of the system of interest [43], [46], [47], [48]. Most vertex models represent a single cross-section of an epithelial sheet, which can be either a ‘generic’ representative cross-section, or explicitly the apical surface of the epithelium, where many of the molecular regulators of interest are thought to be localized. In this representation, sheets are reduced to two dimensions, where cells are polygons, interfaces between cells are straight lines, and vertices are the points where three (or more) interfaces meet. As such, this representation includes an explicit description of the cell shape (although it does not typically allow for curved cell edges), and analytically, the complete configuration of the tissue is determined by the 2-dimensional positions of the vertices and their connectivity.

Current vertex models for epithelia trace their origins in the physical description of foams and bubbles. The equilibrium configuration of the foam is the configuration that minimizes the bubbles’ surface tension energy relative to their surface area, and were the basis for the first analogous models for epithelial cells [49]. Thus, in addition to the vertex-meshwork description of the tissue configuration, vertex models for epithelia are accompanied by equations that determine the directions and magnitudes of the forces.

One way to employ these models for force estimation is to use the classical assumption that the tissue is in instantaneous equilibrium. Since the forces are assumed to be balanced, the tissue geometry can be used for mechanical stress inference. Recent studies have proposed

different strategies to develop inverse problem frameworks to estimate cell pressures and interface tensions from the observed geometry of the cells [50], [51]. It is also possible to drop the equilibrium assumption to allow the tissue to evolve dynamically over time, which is of particular interest for models of dynamic morphogenetic processes. Most models evolve tissue configuration through the independent motion of the vertices, which are combined with some rules for changes in cell connectivity (e.g. through formation and resolution of higher-order vertices). The total force on the vertices can be calculated explicitly [52], [53], but another approach popular with biophysicists is to calculate the forces as the gradient of a Hamiltonian energy function (a fairly detailed discussion of the relevant energy is available, e.g. in [54] or in [55]). In both types of approaches, the vertices are assumed to be embedded in a viscous fluid that resists deformation, i.e. in a friction-dominated environment. As a result, the vertex displacement in a small-time increment (i.e. its velocity) is proportional to the net force.

The functional difference in different epithelial and/or morphogenetic models stems from the choice of forces (or energy terms) that are explicitly included in the model; these can include tension or elastic forces (produced by the cell's actomyosin cortex), cell-cell adhesion (produced by adherens junctions), hydrostatic pressure, and often some type of membrane conservation (elastic or otherwise) (Fig. 5). These forces can either act exclusively in directions parallel to the cell periphery, and thus represent interface tension forces, or models can allow forces to point inwards (i.e. radially) towards cell centroids (such as pressure forces). Through placing additional 'virtual' vertices at cell centers, cell areas can be triangulated in a way that permits the incorporation of viscoelastic elements representing mechanical effects of cytoskeletal components, including 'plastic' active remodeling [43], [46], [56], [57], [58]. Finally, models can also have external tissue forces added on top of the cellular forces [59].

While most vertex models evolve tissue configuration through the independent motion of the vertices, there are alternative strategies. In self-propelled Voronoi models, the epithelial tissue evolves through displacement of cell centroids. Vertices - instead of being treated as independent degrees of freedom - are produced from the position of cell centroids through Voronoi tessellation (e.g. [60], [61], [62]). These types of models rely on the core assumption that tissue conformations correspond closely to a Voronoi tessellation with cell centers acting as Voronoi seeds. This implies that cell-cell interfaces maximize their distances to cell centroids in an isotropic fashion, which may not always be the case in planar-polarized developmental systems. However, these models have key advantages due to their reduced computational complexity, as displacing centroids is computationally more efficient than tracking vertices. Additionally, topological changes do not have to be explicitly coded into the computational model but instead occur naturally from the Voronoi tessellation of the existing centroids.

Relationship Between Tissue Morphology and Physical Properties

One important goal in cellular models of morphogenesis, in particular that of vertex models, is to infer the balance between tension forces from the observed morphology of the tissue. In simple packing geometries – such as the drosophila eye epithelium - these relationships can

be inferred fairly directly from the cellular configurations (e.g. [63]); however, many epithelial vertex models address the issue of morphology by borrowing further from the physics of foams and polymers. Specifically, it has been proposed that epithelial tissues can exhibit ‘glassy’ behavior; this means that tissues can undergo transition between a more elastic solid-like state (in which the tissue configuration represents the local energy minimum, and work is required to compress, expand or shear the tissue from its equilibrium position) and a more ‘soft’, or fluid-like, state (that is ‘degenerate’, which means that there are multiple states with the same minimal energy that causes the shear resistance to disappear, so that cells can easily move past each other). In the solid-like state, tissue morphologies are typically more regular and ordered, while in softer states, cell morphologies are more irregular and disordered. The approach to infer elastic properties from epithelial tissue morphology has been discussed in particular detail in Farhadifar et al. 2007 [58]. This general framework has been used to propose that shape changes accompany fluid-to-solid transition in proliferating tissue [64]. It has also been proposed that the transition from solid-like to fluid-like state in epithelia is controlled by competition between cell-cell adhesion and cortical tension, which is characterized by a shape index such that cell shape and tissue morphology constitute a specific readout for the glass transition [60], [61]. This approach was also used to examine the relationship between cell shape and mechanical stress at the cell and tissue level [65].

Importantly, in morphological processes such as intercalation, there are significant energy barriers to cell rearrangement. This means that, while the endpoint of a remodeling process (such as the T3 configuration) may be energetically more favorable than the starting point (such as the T1 configuration), the energy associated with the geometric transition between these two points (the T2 configuration) is not smooth. Instead, the T2 configuration is energetically more unfavorable than either T1 or T3. This means that energy has to be temporarily ‘injected’ into the system in order to overcome this barrier. Since the research cited above posits that these energy barriers to tissue remodeling disappear for increased cell-cell adhesion, or for decreased contractility, these studies suggest that modulation of these parameters can contribute to overcoming the energy barrier. It has also been suggested that these ‘injections’ can come from system noise, such as active contractions of cell cortex driven by junctional Myosin II, which thus creates something like an active ‘fluidization’ [66].

Intercalation in vertex models in GBE

In the framework of computational models, cell intercalation necessarily requires topological transitions from T1 to T3, i.e. the shrinkage of a T1 interface between AP-neighboring cells into a higher-order vertex, and its subsequent resolution into a T3 interface between two DVneighboring cells. While, in theory, cell intercalation in epithelia can arise passively as the tissue is stretched by external forces [59], intercalation during GBE is actively-driven by cell-autonomous processes [23]. Quantitative vertex models can be used to cast cell intercalation into an analytical framework, and these have been used to combine elements of tensor analysis and continuum mechanics to measure strain rates in intercalation [25].

In addition, vertex models can be adapted in a straightforward fashion to incorporate the experimentally-defined properties of key morphogenetic proteins at cell interfaces – the function of these proteins is thought to convey spatially anisotropic interface tension. Anisotropic tension in the vertex model has been implemented in computational simulations of tissue intercalation [17], [59]. Specifically, assigning higher line tensions at AP interfaces based on their spatial orientation (and thus making them energetically less favorable) causes contraction of these interfaces into higher-order vertices (i.e. the T2 configuration), and produces the resolution of higher-order vertices into T3 interfaces (with the additional implementation of inhibiting T1 reelongation). These simulations can also incorporate additional external forces to produce different cell morphologies and T3 orientations [23]. This conceptual approach was also used to simulate intercalation behavior with interface tensions depending on specific ‘identities’ of adjacent cells [67].

This approach has been further refined in chemo-mechanical models [68], [69]. These models include planar polarized interface tension, but also include an explicit energy term for ‘spokes’, which are the lines connecting vertices to the cell centroid. These spokes represent actin cables on which Myosin II pulses can be imposed to represent cyclical medial myosin activation and thereby produce cell area oscillations. In addition, time-dependent tension values are assigned based on experimental estimates of the temporal recruitment of planar polarity proteins, including a positive feedback mechanism for Myosin II. Interestingly, in these models anisotropic contractile forces still drive intercalation, but while junctional Myosin II (and thus interface tensions) were relevant for the contraction of AP interfaces, it was found that the spoke-like, medial Myosin II tension was relevant for DV interface elongation.

Accommodating non-polygonal cell shapes

In most vertex models, the cellular polygons are defined by cell-cell interfaces, and conversely, the interfaces are defined as the Euclidian distances between individual vertices. This is a conceptual simplification that matches most central assumptions of vertex models for morphogenesis, especially if interface tensions are assumed to be essential drivers of cell and tissue deformations. However, in cases where tissues develop non-polygonal morphologies, with distinctly rounded and bulging cell outlines, it becomes interesting to question whether mechanistic features may be missed in these models. Aside from the previously mentioned cellular Potts models, which naturally include varied cell shapes, some studies have also tried to expand vertex models to incorporate more information about non-straight cell outlines. For example, some studies have moved toward ‘polyline’ instead of ‘monoline’ models, where individual straight-line interfaces are broken down into shorter line segments through introduction of additional ‘virtual’ vertices placed on the cell boundary. These additional vertices can then be used to ‘attach’ stiff springs, as a formal representation of adherens junctions, so that they allow a more explicit inclusion of adhesion and membrane elasticity [70]. Alternatively, they can be used to attach additional orthogonal dashpots to model viscoelastic properties of the cytosol [71]. Either way, the polyline approach can represent more complex boundary shapes and may allow more fluid and biologically realistic behavior. A third approach has been to approximate curved cell

interfaces as circle segments or chords, which are characterized by a single curvature radius [51].

3-dimensional models for epithelial deformation

3-dimensional models are crucial for comprehensive descriptions of morphogenetic systems where the macroscopic deformation is not planar (as has been modeled in intercalation to date), but consists of the epithelial sheet buckling out of the plane (as e.g. in furrow formation). Indeed, attempts towards quantitative approaches to this problem go back to Odell et al., 1981 [56]. While this problem can also be addressed with finite element continuum approaches [72], which are successful in macroscopically reproducing multiple modes of mesoderm remodeling (including ventral furrow and cephalic furrow invaginations), many studies have focused on adapting true 2D vertex models to explicitly include 3D positional information. One group [73] addressed the issue by ‘rotating’ the classical two-dimensional vertex model for furrow invagination, so that their computational model represents cells in the 2-dimensional plane spanned by the dorsal-ventral and the apical-basal axis (instead of the plane spanned by the dorsal-ventral and the anterior-posterior axis like most other models) into the plane, allowing explicit deformations of cells along the apical-basal axis; a similar principle was used in [74], [75].

Some of these models achieve their goal with a quasi-2D sheet; this means that the cell configuration is still a polygonal meshwork (representing the cells midsection or apical section), but that the positions of the vertices are defined in 3D. In these models, the emergence of 3D structure is driven by mechanical buckling due to in-plane stresses [76], [77]. However, there are also parsimonious vertex models that explicitly model the cells’ volume, representing cells as 3-dimensional polyhedrons (i.e. prism-like structures). Many of these are based on Okuda’s reversible network reconnection (RNR) model [78], where each vertex connects to exactly four interfaces (three in the AP-DV plane as in 2D models, and one interface into the apical-basal direction). Thus, variants of these models allow behavior at distinct apical and basal surfaces [79], [80].

6. Conclusions and future directions

While studies on cell intercalation have revealed a new capacity for biophysical approaches and interpretations, there is much room to achieve a better understanding of the processes that direct cell intercalation. Integral to this will be better approximations through modeling-based approaches of the mechanisms guiding morphogenesis. The three-dimensionality of cells at these stages has been largely ignored both in experimental and modeling work. Indeed, cells at these stages are deeply columnar epithelia – typically around 7 μm in width, but 30–35 μm in depth. Exploring this will require new modes of imaging, as the lipid-rich embryo suffers from extensive signal extinction at deeper levels. It will be interesting to see if light-sheet microscopy and Bessel beam-based techniques can overcome these limitations. Adaptive-optics approaches may also be useful in addressing these issues. With these imaging modalities, file sizes often become even greater, and terabyte-sized movie sequences are not uncommon. This places an even greater emphasis on computational analysis, and a clear future frontier in such analysis is the application of machine learning

approaches to segmentation and object-recognition. If successful, this will permit volumetric analysis that will drive new hydrodynamic and 3D vertex models. Meaningful 3D models will require the explicit consideration of apical-basal gradients of parameters that have been previously used to generate planar-directed forces in 2D models (for example, cell-cell adhesion, line tension, or fluid pressure forces). However, these models will also need to provide a framework for force components directly into the apical-basal direction. Through these combined approaches, advances in imaging, computational analysis and modeling will lead to a new and deeper understanding of the forces that drive epithelial morphogenesis.

Acknowledgements

The authors declare no competing financial interests. We thank members of the Blankenship and Loerke labs for critical reading and constructive comments on the manuscript. A special thanks to Tim Vanderleest, Hui Miao, and Celia Smits for providing images or illustrations. This work was supported by grants from the NIH NIGMS: R01GM127447 and R15 GM126422 to J.T.B., and NIH R01GM127447 and R15 GM117463 to D.L.

References

[1]. Irvine KD, Wieschaus E, Cell intercalation during Drosophila germband extension and its regulation by pair-rule segmentation genes, Development, 120 (4) (1994), pp. 827–41 [PubMed: 7600960]

[2]. M da Silva S, Vincent JP, Oriented cell divisions in the extending germband of Drosophila, Development, 134 (17) (2007), pp. 3049–54. 10.1242/dev.004911 [PubMed: 17652351]

[3]. Butler LC, Blanchard GB, Kabla AJ, Lawrence NJ, Welchman DP, Mahadevan L, Adams RJ, Sanson B Cell shape changes indicate a role for extrinsic tensile forces in Drosophila germ-band extension, Nat. Cell Biol 11 (7) (2009), pp. 859–64. 10.1038/ncb1894 [PubMed: 19503074]

[4]. Wang MF, Hunter MV, Wang G, McFaul C, Yip CM, Fernandez-Gonzalez R, Automated cell tracking identifies mechanically oriented cell divisions during Drosophila axis elongation, Development, 144 (7) (2017), pp. 1350–1361. 10.1242/dev.141473 [PubMed: 28213553]

[5]. Sun Z, Amourda C, Shagirov M, Hara Y, Saunders TE, Toyama Y, Basolateral protrusion and apical contraction cooperatively drive Drosophila germ-band extension Nat. Cell Biol 19 (4) (2017), pp. 375–383. 10.1038/ncb3497 [PubMed: 28346438]

[6]. Bertet C, Sulak L, Lecuit T Myosin-dependent junction remodelling controls planar cell intercalation and axis elongation Nature, 429 (6992) (2004), pp. 667–71. 10.1038/nature02590 [PubMed: 15190355]

[7]. Blankenship JT, Backovic ST, Sanny JS, Weitz O, Zallen JA Multicellular rosette formation links planar cell polarity to tissue morphogenesis Dev. Cell 11 (2016), pp. 459–70. 10.1016/j.devcel.2006.09.007

[8]. Zallen JA, Wieschaus E Patterned gene expression directs bipolar planar polarity in Drosophila Dev. Cell 6 (3) (2004), pp. 343–55. 10.1016/s1534-5807(04)00060-7 [PubMed: 15030758]

[9]. Rauzi M, Lenne PF, Lecuit T Planar polarized actomyosin contractile flows control epithelial junction remodelling Nature, 468 (2010), pp. 1110–1114. 10.1038/nature09566 [PubMed: 21068726]

[10]. Fernandez-Gonzalez R, Zallen JA Oscillatory behaviors and hierarchical assembly of contractile structures in intercalating cells Phys. Biol 8 (4) (2011), 045005. 10.1088/1478-3975/8/4/045005 [PubMed: 21750365]

[11]. Sawyer JK, Choi W, Jung KC, He L, Harris NJ, Peifer M A contractile actomyosin network linked to adherens junctions by canoe/afadin helps drive convergent extension MBoC. 22 (2011), pp. 2491–2508. 10.1091/mbc.E11-05-0411 [PubMed: 21613546]

[12]. Vanderleest TE, Smits CM, Xie Y, Jewett CE, Blankenship JT, Loerke D Vertex sliding drives intercalation by radial coupling of adhesion and actomyosin networks during Drosophila germband extension Elife. 7 (2018) 34586. 10.7554/eLife.34586

[13]. Simões SM, Blankenship JT, Weitz O, Farrell DL, Tamada M, Fernandez-Gonzalez R, Zallen JA Rho-kinase directs Bazooka/Par-3 planar polarity during Drosophila axis elongation Dev. Cell 19 (3) (2010), pp. 377–88. 10.1016/j.devcel.2010.08.011 [PubMed: 20833361]

[14]. Martin AC, Kaschube M, Wieschaus EF Pulsed contractions of an actin-myosin network drive apical constriction Nature, 457 (7228) (2009), pp. 495–9. 10.1038/nature07522 [PubMed: 19029882]

[15]. Leung CY, Fernandez-Gonzalez R Quantitative image analysis of cell behavior and molecular dynamics during tissue morphogenesis Methods Mol. Biol 1189 (2015), pp. 99–113. 10.1007/978-1-4939-1164-6_7 [PubMed: 25245689]

[16]. Jewett CE, Vanderleest TE, Miao H, Xie Y, Madhu R, Loerke D, Blankenship JT Planar polarized Rab35 functions as an oscillatory ratchet during cell intercalation in the Drosophila epithelium Nat. Commun 8 (1) (2017), 476. 10.1038/s41467-017-00553-0 [PubMed: 28883443]

[17]. Rauzi M, Verant P, Lecuit T, Lenne PF Nature and anisotropy of cortical forces orienting Drosophila tissue morphogenesis Nat. Cell Biol 12 (12) (2008), pp. 1401–10. 10.1038/ncb1798

[18]. Farrell DL, Weitz O, Magnasco MO, Zallen JA SEGGA: a toolset for rapid automated analysis of epithelial cell polarity and dynamics Development, 144 (9) (2017), pp. 1725–1734. 10.1242/dev.146837 [PubMed: 28465336]

[19]. Etournay R, Merkel M, Popović M, Brandl H, Dye NA, Aigouy B, Salbreux G, Eaton S, Jülicher F TissueMiner: A multiscale analysis toolkit to quantify how cellular processes create tissue dynamics Elife, 5 (2016), e14334. 10.7554/eLife.14334 [PubMed: 27228153]

[20]. Huet S, Karatekin E, Tran VS, Fanget I, Cribier S, Henry JP Analysis of transient behavior in complex trajectories: application to secretory vesicle dynamics Biophys. J 91 (2006), pp. 3542–3559. 10.1529/biophysj.105.080622 [PubMed: 16891360]

[21]. Hsu M-K, Sheu JC, Hsue C Overcoming the negative frequencies: instantaneous frequency and amplitude estimation using osculating circle method J. Marine Science and Technology 19 (2011), pp. 514–521

[22]. Fernandez-Gonzalez R, Simoes SM, Röper JC, Eaton S, Zallen JA Myosin II dynamics are regulated by tension in intercalating cells Dev. Cell 17 (5) (2009), pp. 736–43. 10.1016/j.devcel.2009.09.003 [PubMed: 19879198]

[23]. Collinet C, Rauzi M, Lenne PF, Lecuit T Local and tissue-scale forces drive oriented junction growth during tissue extension Nat. Cell Biol 17 (10) (2015), pp. 1247–58. 10.1038/ncb3226 [PubMed: 26389664]

[24]. Yu JC, Fernandez-Gonzalez R Local mechanical forces promote polarized junctional assembly and axis elongation in Drosophila Elife. 5 (2016), e10757. 10.7554/eLife.10757 [PubMed: 26747941]

[25]. Blanchard GB, Kabla AJ, Schultz NL, Butler LC, Sanson BN, Gorfinkiel B,N, Mahadevan L, Adams RJ Tissue tectonics: morphogenetic strain rates, cell shape change and intercalation. Nat. Methods, 6 (6) (2009) pp. 458–64. 10.1038/nmeth.1327 [PubMed: 19412170]

[26]. Kale GR, Yang X, Philippe JM, Mani M, Lenne PF, Lecuit T Distinct contributions of tensile and shear stress on E-cadherin levels during morphogenesis Nat. Commun 9 (1) (2018), 5021. 10.1038/s41467-018-07448-8 [PubMed: 30479400]

[27]. Munjal A, Lecuit T Actomyosin networks and tissue morphogenesis Development, 141 (9) (2014), pp. 1789–93. 10.1242/dev.091645 [PubMed: 24757001]

[28]. He B, Doubrovinski K, Polyakov O, Wieschaus E Apical constriction drives tissue-scale hydrodynamic flow to mediate cell elongation Nature, 508 (7496) (2014), pp. 392–6. 10.1038/nature13070 [PubMed: 24590071]

[29]. Desprat N, Supatto W, Pouille PA, Beaurepaire E, Farge E Tissue deformation modulates twist expression to determine anterior midgut differentiation in Drosophila embryos Dev. Cell 15 (3) (2008), pp. 470–7. 10.1016/j.devcel.2008.07.009 [PubMed: 18804441]

[30]. Doubrovinski K, Swan M, Polyakov O, Wieschaus EF Measurement of cortical elasticity in Drosophila melanogaster embryos using ferrofluids Proc Natl Acad Sci U S A. 114 (5) (2017), pp. 1051–1056. 10.1073/pnas.1616659114 [PubMed: 28096360]

[31]. Serwane F, Mongera A, Rowghanian P, Kealhofer DA, Lucio AA, Hockenbery ZM, Campàs O In vivo quantification of spatially varying mechanical properties in developing tissues Nat. Methods 14 (2) (2017), pp. 181–186. 10.1038/nmeth.4101 [PubMed: 27918540]

[32]. Mongera A, Rowghanian P, Gustafson HJ, Shelton E, Kealhofer DA, Carn EK, Serwane F, Lucio AA, Giammona J, Campàs O A fluid-to-solid jamming transition underlies vertebrate body axis elongation Nature, 561 (7723) (2018), pp. 401–405. 10.1038/s41586-018-0479-2 [PubMed: 30185907]

[33]. Wessel AD, Gumalla M, Grosshans J, Schmidt CF The mechanical properties of early Drosophila embryos measured by high-speed video microrheology Biophys. J 108 (8) (2015), pp. 1899–907. 10.1016/j.bpj.2015.02.032 [PubMed: 25902430]

[34]. Clément R, Dehapiot B, Collinet C, Lecuit T, Lenne PF Viscoelastic Dissipation Stabilizes Cell Shape Changes during Tissue Morphogenesis Curr. Biol 27 (20) (2017), pp. 3132–3142. 10.1016/j.cub.2017.09.005 [PubMed: 28988857]

[35]. Levayer R, Pelissier-Monier A, Lecuit T Spatial regulation of Dia and Myosin-II by RhoGEF2 controls initiation of E-cadherin endocytosis during epithelial morphogenesis Nat. Cell Biol 13 (5) (2011), pp. 529–40. 10.1038/ncb2224 [PubMed: 21516109]

[36]. Roh-Johnson M, Shemer G, Higgins CD, McClellan JH, Werts AD, Tulu US, Gao L, Betzig E, Kiehart DP, Goldstein B Triggering a cell shape change by exploiting preexisting actomyosin contractions Science, 335 (2012), pp. 1232–1235. 10.1126/science.1217869 [PubMed: 22323741]

[37]. Simões S, Oh Y, Wang MFZ, Fernandez-Gonzalez R, Tepass U Myosin II promotes the anisotropic loss of the apical domain during Drosophila neuroblast ingression J. Cell Biol 216 (5) (2017), pp. 1387–1404. 10.1083/jcb.201608038. [PubMed: 28363972]

[38]. An Y, Xue G, Shaobo Y, Mingxi D, Zhou X, Yu W, Ishibashi T, Zhang L, Yan Y Apical constriction is driven by a pulsatile apical myosin network in delaminating Drosophila neuroblasts Development, 144 (2017), pp. 2153–2164. 10.1242/dev.150763 [PubMed: 28506995]

[39]. Brodland GW How computational models can help unlock biological systems Semin. Cell Dev. Biol 47–48 (2015), pp. 62–73. 10.1016/j.semcdb.2015.07.001

[40]. Ishihara S, Marcq P, Sugimura K From cells to tissue: A continuum model of epithelial mechanics Phys. Rev. E 96 (2–1) (2017), 022418. 10.1103/PhysRevE.96.022418 [PubMed: 28950595]

[41]. Derganc J, Svetina S, Zeks B Equilibrium mechanics of monolayered epithelium J. Theor. Biol 260 (3) (2009), pp. 333–9. 10.1016/j.jtbi.2009.06.021 [PubMed: 19576229]

[42]. Okuda S, Inoue Y, Eiraku M, Adachi T, Sasai Y Vertex dynamics simulations of viscosity-dependent deformation during tissue morphogenesis Biomech. Model Mechanobiol 14 (2) (2015), pp. 413–25. 10.1007/s10237-014-0613-5 [PubMed: 25227116]

[43]. Brodland GW Computational modeling of cell sorting, tissue engulfment, and related phenomena: A review Appl. Mech. Rev 57 (1) (2004), pp. 47–76

[44]. Zajac M, Jones GL, Glazier JA Model of convergent extension in animal morphogenesis Phys. Rev. Lett 85 (9) (2000), pp. 2022–5. 10.1103/PhysRevLett.85.2022 [PubMed: 10970673]

[45]. Zajac M, Jones GL, Glazier JA Simulating convergent extension by way of anisotropic differential adhesion J. Theor. Biol 222 (2) (2003), pp. 247–59. 10.1016/s0022-5193(03)00033-x [PubMed: 12727459]

[46]. Fletcher AG, Osterfield M, Baker RE, Shvartsman SY Vertex models of epithelial morphogenesis Biophysical Journal, 106 (11) (2014), pp. 2291–304. 10.1016/j.bpj.2013.11.4498 [PubMed: 24896108]

[47]. Alt S, Ganguly P, Salbreux G Vertex models: from cell mechanics to tissue morphogenesis Philos. Trans. R. Soc. Lond. B. Biol. Sci 372 (1720) (2017), 20150520. 10.1098/rstb.2015.0520 [PubMed: 28348254]

[48]. Fletcher AG, Cooper FC, Baker RE Mechanocellular models of epithelial morphogenesis Philos. Trans. R. Soc. Lond. B. Biol. Sci 372 (1720) (2017), 20150519. 10.1098/rstb.2015.0519 [PubMed: 28348253]

[49]. Honda H, Eguchi G How much does the cell boundary contract in a monolayered cell sheet?J. Theor. Biol 84 (3) (1980), pp. 575–88. 10.1016/s0022-5193(80)80021-x [PubMed: 7431941]

[50]. Ishihara S, Sugimura K Bayesian inference of force dynamics during morphogenesis J. Theor. Biol 313 (2012), pp. 313:201–11. 10.1016/j.jtbi.2012.08.017 [PubMed: 22939902]

[51]. Chiou KK, Hufnagel L, Shraiman BI Mechanical Stress Inference for Two Dimensional Cell Arrays PLoS Comput. Biol 8 (5) (2012), e1002512. 10.1371/journal.pcbi.1002512 [PubMed: 22615550]

[52]. Weliky M, Oster G The mechanical basis of cell rearrangement. I. Epithelial morphogenesis during Fundulus epiboly Development, 109 (2) (1990), pp. 373–86 [PubMed: 2401201]

[53]. Hutson MS, Veldhuis J, Ma X, Lynch HE, Cranston PG, Brodland GW Combining Laser Microsurgery and Finite Element Modeling to Assess Cell-Level Epithelial Mechanics Biophys. J 97 (12) (2009), pp. 3075–3085. 10.1016/j.bpj.2009.09.034 [PubMed: 20006944]

[54]. Hiraiwa T, Kuranaga E, Shibata T Wave Propagation of Junctional Remodeling in Collective Cell Movement of Epithelial Tissue: Numerical Simulation Study Front. Cell Dev. Biol 5 (2017), pp. 66. 10.3389/fcell.2017.00066 [PubMed: 28770197]

[55]. Spencer MA, Jabeen Z, Lubensky DK Vertex stability and topological transitions in vertex models of foams and epithelia Eur. Phys. J. E. Soft Matter, 40 (1) (2017), 2. 10.1140/epje/i2017-11489-4 [PubMed: 28083791]

[56]. Odell GM, Oster G, Alberch P, Burnside B The mechanical basis of morphogenesis. I. Epithelial folding and invagination Dev. Biol 85 (2) (1981), pp. 446–62. 10.1016/0012-1606(81)90276-1 [PubMed: 7196351]

[57]. Brodland GW, Chen HH The mechanics of heterotypic cell aggregates: insights from computer simulations J. Biomech. Eng 122 (4) (2000), pp. 402–7. 10.1115/1.1288205 [PubMed: 11036564]

[58]. Farhadifar R, Röper JC, Aigouy B, Eaton S, Jülicher F The influence of cell mechanics, cell-cell interactions, and proliferation on epithelial packing.Current Biology, 17 (24) (2007), pp. 2095–104. 10.1016/j.cub.2007.11.049 [PubMed: 18082406]

[59]. Honda H, Nagai T, Tanemura M Two different mechanisms of planar cell intercalation leading to tissue elongation Dev. Dyn 237 (7) (2008), pp. 1826–36. 10.1002/dvdy.21609 [PubMed: 18570249]

[60]. Bi D, Lopez JH, Schwarz JM, Manning ML A density-independent rigidity transition in biological tissues Nature Physics, 11 (2015), pp. 1074–1079. 10.1038/nphys3471

[61]. Yang X, Bi D, Czajkowski M, Merkel M, Manning ML, Marchetti MC Correlating cell shape and cellular stress in motile confluent tissues PNAS. 114 (48) (2017), pp. 12663–12668. 10.1073/pnas.1705921114 [PubMed: 29138312]

[62]. Barton DL, Henkes S, Weijer CJ, Sknepnek R Active Vertex Model for cell-resolution description of epithelial tissue mechanics PLoS Comput. Biol 13 (6) (2017), e1005569. 10.1371/journal.pcbi.1005569 [PubMed: 28665934]

[63]. Hilgenfeldt S, Erisken S, Carthew RW Physical modeling of cell geometric order in an epithelial tissue PNAS, 105 (3) (2008), pp. 907–911. 10.1073/pnas.0711077105 [PubMed: 18192402]

[64]. Puliafito A, Hufnagel L, Neveu P, Streichan S, Sigal A, Fygenson DK, Shraiman BI Collective and single cell behavior in epithelial contact inhibition PNAS. 109 (3) (2012), pp. 739–44. 10.1073/pnas.1007809109 [PubMed: 22228306]

[65]. Nestor-Bergmann A, Goddard G, Woolner S, Jensen OE Relating cell shape and mechanical stress in a spatially disordered epithelium using a vertex-based model Math. Med. Biol 35 (2018), pp. 1–27. 10.1093/imammb/dqx008

[66]. Krajnc M, Dasgupta S, Ziherl P, Prost J Fluidization of epithelial sheets by active cell rearrangements Phys. Rev. E 98 (2–1) (2018), 022409. 10.1103/PhysRevE.98.022409 [PubMed: 30253464]

[67]. Tetley RJ, Blanchard GB, Fletcher AG, Adams RJ, Sanson B Unipolar distributions of junctional Myosin II identify cell stripe boundaries that drive cell intercalation throughout Drosophila axis extension Elife. 5 (2016) 12094. 10.7554/eLife.12094

[68]. Lan H, Wang Q, Fernandez-Gonzalez R, Feng JJ A biomechanical model for cell polarization and intercalation during Drosophila germband extension Phys. Biol 12 (5) (2015), 056011. 10.1088/1478-3975/12/5/056011 [PubMed: 26356256]

[69]. Siang LC, Fernandez-Gonzalez R, Feng JJ Modeling cell intercalation during Drosophila germband extension Phys. Biol 15 (6) (2018), 066008. 10.1088/1478-3975/aad865 [PubMed: 30080681]

[70]. Tamulonis C, Postma M, Marlow HQ, Magie CR, de Jong J, Kaandorp J A cell-based model of Nematostella vectensis gastrulation including bottle cell formation, invagination and zippering Dev. Biol 351 (1) (2011), pp. 217–28. 10.1016/j.ydbio.2010.10.017 [PubMed: 20977902]

[71]. Perrone MC, Veldhuis JH, Brodland GW Non-straight cell edges are important to invasion and engulfment as demonstrated by cell mechanics model Biomech. Model Mechanobiol 15 (2) (2016), pp. 405–18. 10.1007/s10237-015-0697-6 [PubMed: 26148533]

[72]. Allena R, Mouronval AS, Aubry D Simulation of multiple morphogenetic movements in the Drosophila embryo by a single 3D finite element model J. Mech. Behav. Biomed. Mater 3 (4) (2010), pp. 313–23. 10.1016/j.jmbbm.2010.01.001 [PubMed: 20346899]

[73]. Hočevar Brezavšček A, Rauzi M, Leptin M, Ziherl P A model of epithelial invagination driven by collective mechanics of identical cells Biophys. J 103 (5) (2012), pp. 1069–77. 10.1016/j.bpj.2012.07.018 [PubMed: 23009857]

[74]. Wen FL, Wang YC, Shibata T Epithelial Folding Driven by Apical or Basal-Lateral Modulation: Geometric Features, Mechanical Inference, and Boundary Effects. Biophys. J 112 (12) (2017), pp. 2683–2695. 10.1016/j.bpj.2017.05.012 [PubMed: 28636924]

[75]. Dasgupta A, Merkel M, Clark MJ, Jacob AE, Dawson JE, Manning ML, Amack JD Cell volume changes contribute to epithelial morphogenesis in zebrafish Kupfferís vesicle eLife, 7 (2018), e30963. 10.7554/eLife.30963 [PubMed: 29376824]

[76]. Osterfield M, Du X, Schupbach T, Wieschaus E, Shvartsman SY Three-dimensional epithelial morphogenesis in the developing Drosophila egg Dev. Cell, 24 (4) (2013), pp. 400–1. 10.1016/j.devcel.2013.01.017 [PubMed: 23449472]

[77]. Du X, Osterfield M, Shvartsman SY Computational analysis of three-dimensional epithelial morphogenesis using vertex models Phys. Biol 11 (6) (2014), 066007. 10.1088/1478-3975/11/6/066007 [PubMed: 25410646]

[78]. Okuda S, Inoue Y, Eiraku M, Sasai Y, Adachi T Reversible network reconnection model for simulating large deformation in dynamic tissue morphogenesis Biomech. Model Mechanobiol 12 (4) (2013), pp. 627–44. 10.1007/s10237-012-0430-7 [PubMed: 22941051]

[79]. Misra M, Audoly B, Kevrekidis IG, Shvartsman SY Shape Transformations of Epithelial Shells Biophys. J 110 (7) (2016), pp. 1670–1678. 10.1016/j.bpj.2016.03.009 [PubMed: 27074691]

[80]. Hannezo E, Prost J, Joanny J Theory of epithelial sheet morphology in three dimensions PNAS, 111 (1) (2014), pp. 27–32. 10.1073/pnas.1312076111 [PubMed: 24367079]

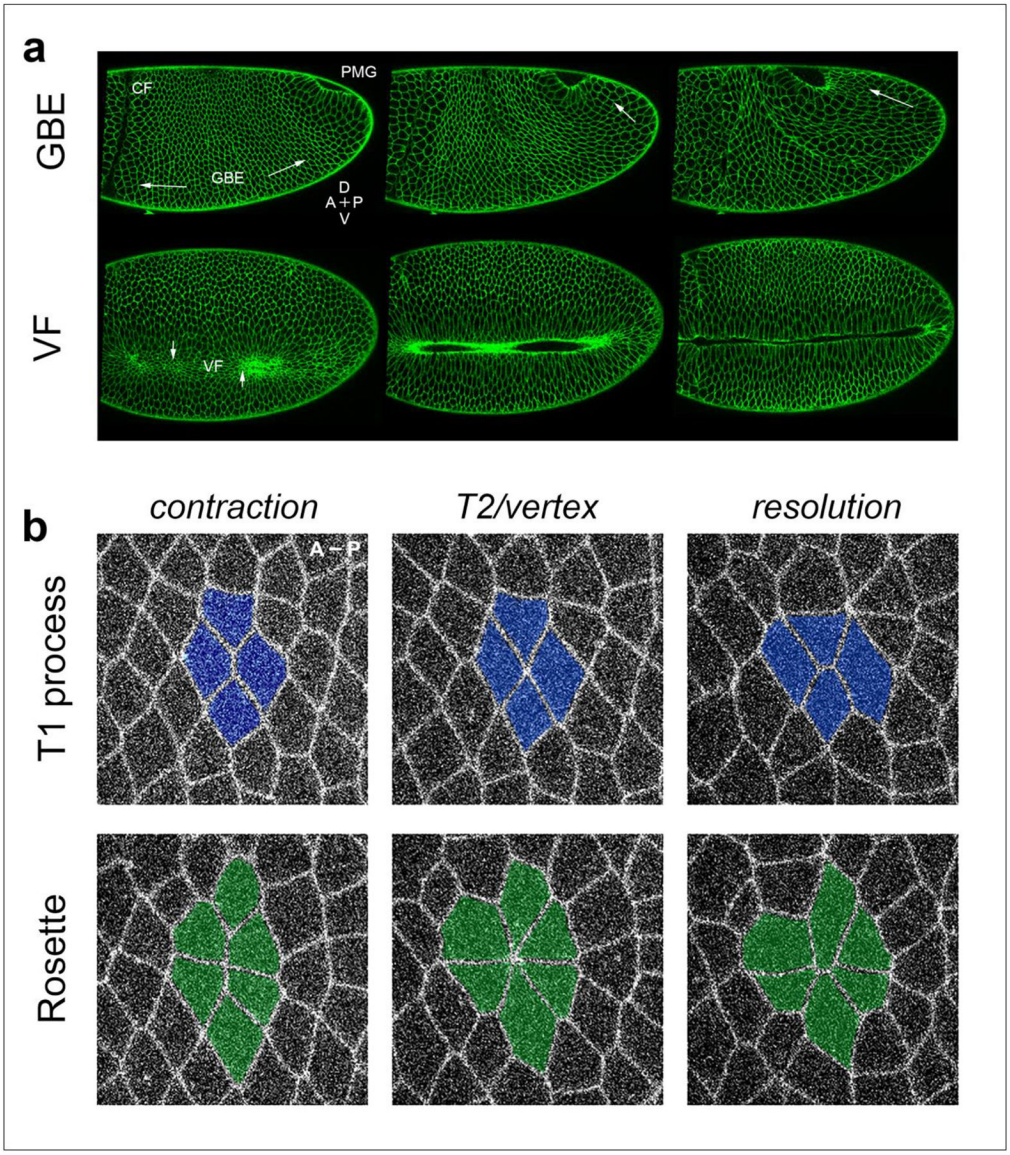

Figure 1. Rearrangements in neighbor cell relationships underlie cell intercalation in the *Drosophila* germband.

(a) Germband extension (GBE) and ventral furrow formation (VF) shown at tissue level low-magnification. The cephalic furrow (CF) and posterior midgut (PMG) are also demarcated. Arrows show direction of cell and tissue displacement, with the germband wrapping around the embryo posterior and continuing to extend along the dorsal surface at later time points (middle and right columns, lateral view of embryo). Similarly, the ventral furrow deepens and invaginates with time (ventrolateral view). The anterior-posterior and dorsal-ventral axes are also indicated. (b) T1 or rosette processes drive tissue extension during fly gastrulation. Cells at the beginning of a T1 or rosette arrangement (left) contract a shared interfaces to reach a T2 or higher-order vertex configuration (middle), before extending a new surface to generate a T3 configuration or rosette resolution (right). The anterior-posterior (A-P) axis is indicated.

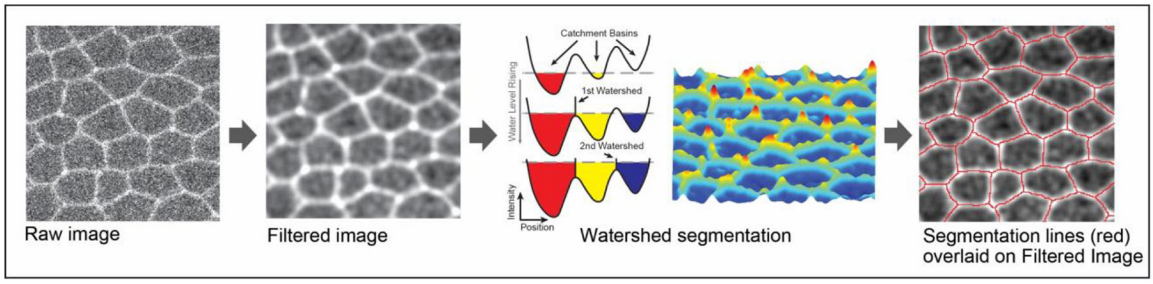

Figure 2. Segmentation workflow for cell analysis.

Raw images are acquired through time-lapse spinning disk confocal microscopy. Images are then Gaussian filtered to fill in small border gaps (usually 1 pixel in size). Images are then segmented by a seeded watershed algorithm. Briefly, local intensity minima form the deepest portion of a catchment basin. As the watershed moves up intensity gradients, where two catchment basins meet a cell boundary is designated (1^{st} and 2^{nd} watersheds). An example of a 3D watershed (x,y, and intensity) is shown to right of line segmentation example. Finally, red lines from segmentation results are imposed on filtered image.

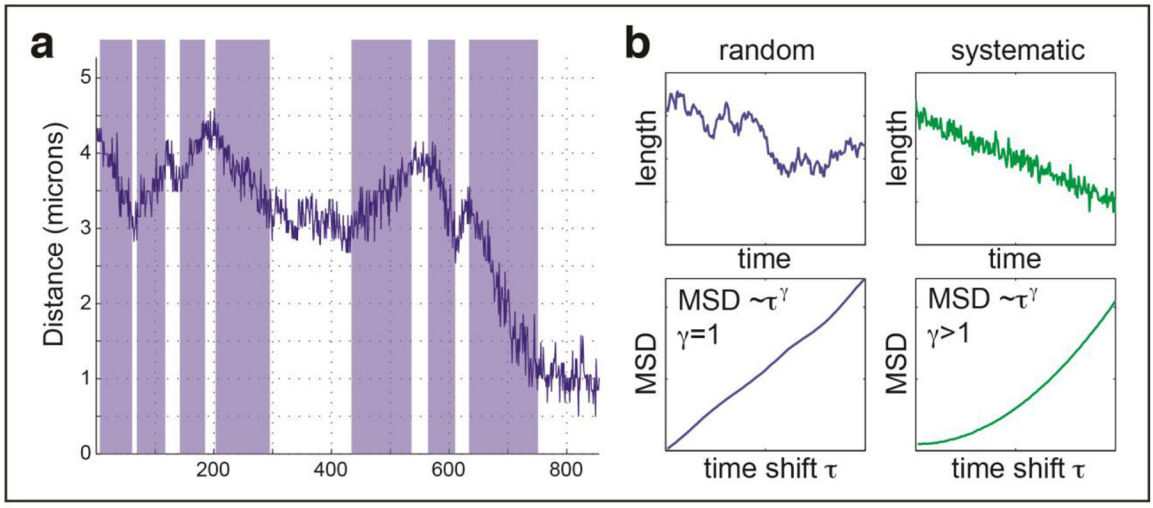

Figure 3. Using Mean Squared Displacements (MSD) trajectories as a quantitative measurement of active motion pulses.

(a) A trace of interface length (y-axis) during a T1 contraction while tracked over an 800 second period (x-axis). Pulses of active motion are shaded in blue as determined by an MSD-based criteria in the which the rolling window possesses a $\gamma>1$. (b) Illustrations of random versus systematic movement. Top panels: Left: Sample of a random-walk length trajectory. Right: Sample of a trajectory with systematic contraction overlaid with noise. Bottom panels: Corresponding Mean Squared Displacements (MSD). A random walk produces an MSD that depends linearly on the time shift tau; the systematic contraction (active motion) produces an MSD that depends superlinearly on the time shift tau (curves upward).

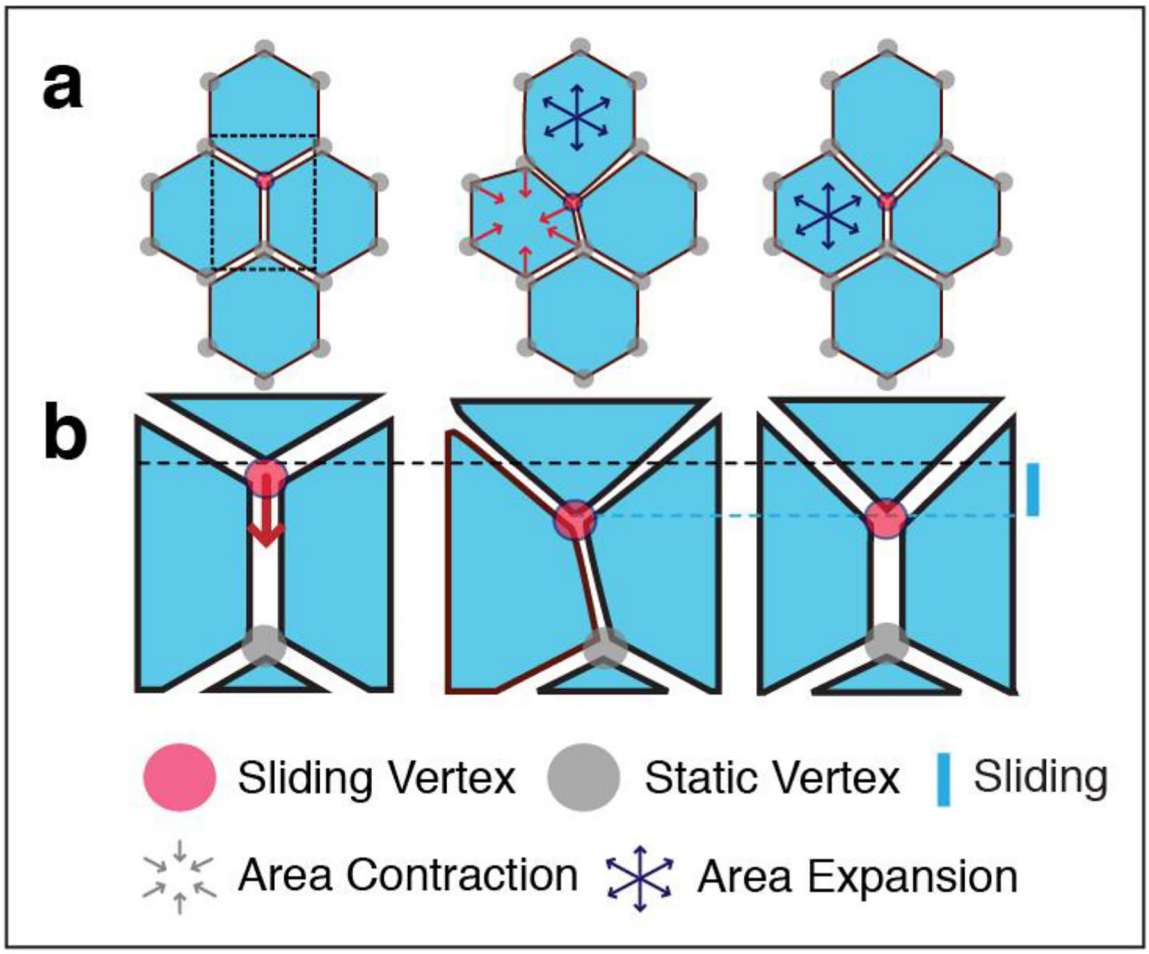

Figure 4. Sliding vertex model for directing changes in cell topologies.

(a) Epithelial cells undergo cyclic expansions and contractions in cell area. These radially-directed forces can be coupled to cell vertices such that when one cell expands (blue arrows) while another cell contracts (red arrows) this can lead to the sliding of a tricellular vertex along the cell periphery. This produces (in this example) the contraction of a vertical T1 interface. (b) A true sliding event (cyan line) will preserve overall interface lengths, such that the shortening of the T1 interface occurs coincident with the lengthening of an associated transverse interface.

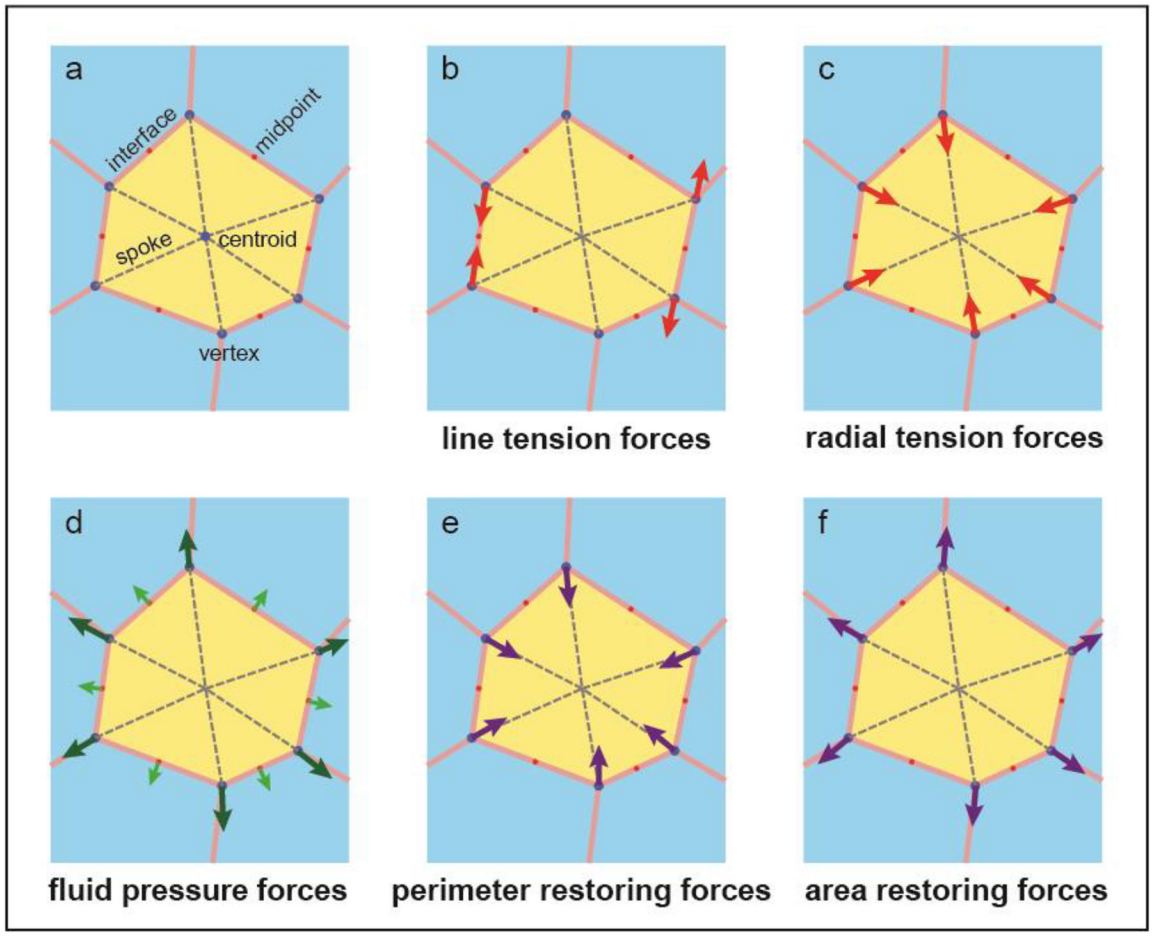

Figure 5. Modeling of force generation in an epithelial cell.

(a) Schematic of a representative hexagonal cell (yellow), showing vertices and the cell centroid, interfaces, interface midpoints, and 'spokes' connecting the vertices with the centroid. (b) Line tension forces on vertices are directed parallel to the interface in question. For an increase in actomyosin line tension in the interface, the forces are pulling inwards towards the interface midpoint; for an increase of adhesion, the tension forces point outward. (c) Radial tension forces on vertices, such as generated by medial/apical actomyosin contraction, are assumed to be directed towards the cell centroid. (d) Pressure forces are exerted isotropically in all directions, and can be thought to generate small identical forces vectors perpendicular to the interfaces along the full interface length. As a result, the net pressure force acting on a vertex is into the direction bisecting the inner vertex angle -- this direction is not necessarily perfectly parallel to the radial spoke pointing to the centroid. (e) Perimeter restoring forces are the result of the perimeter conservation (or minimization) term in the Hamiltonian energy function, which conceptually represents elastic surface conservation of the 3-dimensional cell. Since the force is the negative gradient of the potential energy function, one force component points into that direction for which the cell perimeter is reduced the most. As in (d), depending on cell shape, this direction is not perfectly parallel to the radial spoke pointing to the centroid. (f) Area restoring forces are the result of the area conservation term in the Hamiltonian energy function, which conceptually

represents elastic volume conservation of the 3-dimensional cell. As in (e), the force is the negative gradient of the potential energy function, so that one force component points in the direction which brings the cell closest to its target area (pointing outward if the cell is smaller than its target area, and inward if the cell is larger than its target area). Again, depending on morphology, this direction is not necessarily parallel to either the radial spoke, or to the pressure force vector.

Table 1.

Modeling tissue morphogenesis through different approaches.

Model	Conceptual Explanation	Literature Examples
Continuum mechanics	Treat tissue as a continuum material, usually without incorporating cell-level properties	Ishihara et al., 2017 Derganc et al., 2009 Okuda et al., 2015
Lattice-Based (e.g. cellular Potts)	Considers individual cells. Cells are represented by a collection of lattice points (i.e. pixels), and the tissue morphology is evolved through reassignment of edge pixels (performed using rules based on energy minimization).	Zajac et al., 2000 Zajac et al., 2003
Cell-based (e.g. self-propelled Voronoi)	Considers individual cells. Cell centroids can move independently, and interfaces and vertices are generated from cell centroid positions using Voronoi tessellation or similar strategies.	Bi et al., 2016 Yang et al., 2017 Barton et al., 2017
Vertex models	Considers individual cells through a network of vertices interconnected by straight lines. Tissue morphology is evolved through independent motion of vertices; displacement is generated through forces directly acting on vertices, or configurational energy minimization principles.	Honda et al., 1980 Reviewed in: Brodland et al., 2004; Fletcher et al., 2014; Alt et al., 2016; Fletcher et al., 2017
2D Apical-basal Cross-section	The choice of the model's 2-dimensional cross-section is the section at a fixed point along the cells' apical-basal axis. This approach captures the topology within the plane of the sheet, and reveals tissue deformation into the plane of the sheet (e.g. convergent extension), but ignores variation of cellular parameters along apical-basal axis.	Odell et al., 1981 Brodland et al., 2000 Farhadifar et al. 2007 Hilgenfeldt et al., 2008 Rauzi et al., 2008 Blanchard et al., 2009 Collinet et al., 2015 Tetley et al., 2015 Lan et al., 2015 Siang et al., 2018
2D Lateral section cross-section	The choice of the model's 2-dimensional cross-section is the section at a fixed point along the cells' anterior-posterior axis. This approach allows explicit modeling of cell's apical-basal shape, and reveals sheet deformation into the direction normal to the sheet plane (e.g. bending or infolding), but ignores the tissue topology within the plane of the sheet.	Brezavscek et al., 2012 Wen et al., 2017; Dasgupta et al., 2018
3D approaches	3-dimensional information is included either implicitly in a 2-dimensional model (e.g. using bending energy terms), or the tissue is explicitly modeled as 3-dimensional sheet, where cells are polyhedrons (columns) instead of flat polygons.	Odell et al., 1981 Allena et al., 2010 Osterfield et al., 2013; Du et al., 2014 Okuda et al., 2013 Misra et al., 2016; Hannezo et al., 2014 Honda et al., 2008 Krajnc et al., 2018
Non-straight edges	Model is modified to explicitly allow cell-cell interfaces to be described as curved or irregular (instead of straight lines). Cell interfaces can be modeled as circle segments, or as arbitrary shapes using multipoint (polyline) description.	Tamulonis et al., 2011 Perrone et al., 2016 Chiou et al., 2012